Author Copy • Author Copy • Author Copy • Author Copy • Author Copy • Author Copy • Author Copy • Author Copy • Author Copy • Author Copy

Pol. J. Environ. Stud. Vol. 33, No. 5 (2024), 1-10
DOI: *10.15244/pjoes/177463* ONLINE PUBLICATION DATE:

Original Research

Degradation Properties of Sustained Release Membrane Composited of Water-Based Copolymer and Zeolite

Haonan Sun[1], Tao Lei[1*], Xianghong Guo[1], Jianxin Liu[2], Xihuan Sun[1], Juanjuan Ma[1]

[1]College of Water Resource Science and Engineering, Taiyuan University of Technology, Taiyuan 030024, China
[2]College of Chemical Engineering and Technology, Taiyuan University of Technology, Taiyuan 030024, China

Received: 30 March 2023
Accepted: 21 December 2023

Abstract

The self-made slow-release membrane material with water-based copolymer (polyvinyl alcohol PVA, polyvinyl pyrrolidone PVP), zeolite and epoxy resin as raw materials was tested for degradation in buried soil. The effects of soil temperature T (T_{15}, T_{25}, T_{35}) and moisture W (W_{60}, W_{80}, W_{100}) on the degradability of membrane materials were investigated by a comprehensive experimental design, and a hydrothermal coupling model K (T, W) was established. The effects of degradation on the chemical structure, functional groups, and morphology of membrane materials were revealed by infrared spectroscopy and SEM electron microscopy. The results showed that the degradation degree of membrane material was an exponentially positive response to the increase in soil temperature and moisture. The degradation rate of membrane materials under different treatments was 13.7%-17.3%, and the maximum degradation rate was 17.3% under the $T_{35}W_{100}$ condition. The determination coefficient R^2 of the constructed K (T, W) model reached 0.927, and the average relative error of the predicted degradation rate was 1.58%, indicating good accuracy of the model. The infrared spectrum showed that the -OH stretching vibration absorption peak of the degraded membrane becomes wider and the peak intensity increases; the absorption peak intensity of C-H, $-CH_2$, and Si-O weakens; and the peak of the C=C absorption peak appears as a continuous staircase after degradation. The SEM electron microscopy showed there were differences in the pores and cracks of the membrane materials under different treatments, and the degradation was the most obvious under the $T_{35}W_{100}$ condition.

Keywords: water-based copolymer, zeolite, degradation, hydrothermal coupling model

*e-mail: lcsyt@126.com

Author Copy • Author Copy • Author Copy • Author Copy • Author Copy • Author Copy • Author Copy • Author Copy • Author Copy • Author Copy

Introduction

Slow and controlled-release fertilizer can reduce nutrient release rates, greatly improve fertilizer utilization rates, and reduce environmental pollution and economic loss [1, 2]. However, some slow-controlled release fertilizers are difficult to degrade in soil [3]. The degradation characteristics of slow-release membrane materials are directly related to the slow-release effect of fertilizer and the ecological effect of the soil environment [4]. Therefore, it is of great practical significance to study the degradation performance of membrane materials.

The coating materials with inorganic minerals such as white wax, rosin, and sulfur as the main raw materials have poor sustained release and mechanical properties [5, 6]. Phenolic resin, polyacrylic acid, polyurethane, polyolefin, and polyester organic materials have good mechanical properties and slow release properties, but they are difficult to degrade and cause some environmental pollution [7-9]. The exploration and preparation of environment-friendly, degradable, sustained-release membrane materials has become a hot issue to be solved in social development. The polyvinyl alcohol and polyvinylpyrrolidone used in this paper have good film-forming ability, environmental protection, and degradation [10, 11]. Zeolite is widely available and inexpensive [12, 13]. The components of membrane materials are closely related to their degradation characteristics. The components of membrane materials in this paper are different from those in previous studies, and the degradation characteristics may be quite different, which needs to be further clarified. Previous studies have studied the degradation characteristics of membrane materials under different conditions of moisture [14] and degradation duration [15], and it was clear that the degradation rate of hemp fiber film was the fastest under a 25% soil moisture condition, and most of the acetate-starch film can be degraded after 150 days. However, earlier studies did not take into account the effect of soil temperature on degradation characteristics, and the effect of soil temperature-moisture coupling on membrane material degradation was still unknown. The degradation model construction can be used to precisely quantify the relationship between the degradation rate constant of membrane materials and the single factor effect of soil temperature and water [16]. However, the single temperature or water degradation model fails to quantitatively reflect the influence of the soil temperate-water coupling effect on membrane material degradation rate, which needs to be investigated further.

The purpose of this research was to explore the influence of soil temperature, moisture, and their coupling effects on the degradation rate of membrane materials, to reveal the influence of each factor level on the morphology and structure of membrane material degradation, and to build a soil hydrothermal coupling model of membrane material degradation.

Materials and Methods

Materials

PVA 1799 (analytically pure) and PVP K30 (analytically pure) were purchased from Sinopharm Chemical Reagent Co., Ltd. (Shanghai, China). The average polymerization degree of PVA was 1700, and the alcoholysis degree was 98%~99%. The molecular weight of PVP was 45000~58000. 4A zeolite (industrial grade) was purchased from China Shan-xi Taiheng Technology Co., Ltd. (Jinzhong, China). Industrial 4A zeolite was a cage-connected structure consisting of 8 cubic octahedrons and 12 regular tetrahedrons formed by silicon-aluminum oxygen tetrahedral units, belonging to the cubic crystal system. The parameters of 4A zeolite were as follows: Specific surface area; 510 m^2/g; whiteness >95%; apparent density, 0.3~0.5 g/cm^3; average particle size, 2 um. PVA, PVP, and zeolite are non-polluting and environmentally friendly materials that can degrade under natural conditions and belong to environment-friendly materials. Epoxy resin (industrial grade) was purchased from China Shandong Yousuo Chemical Technology Co., Ltd. (Linyi, China). It could be toxic to the soil if used in excess. The soil texture was sandy loam. The parameters of the soil were as follows: field water holding capacity, 0.226 g/g; bulk density, 1.43 g/cm^3; PH, 8.43; organic matter, 15.32 g/kg; total nitrogen, 1.12 g/kg; alkaline nitrogen, 52.21 mg/kg; available phosphorus, 22.31 mg/kg; and available potassium, 120.32 mg/kg.

Fabrication of Membrane

Weigh PVA with a mass of 51.1 g and deionized water with a mass of 626.5 g in a three-necked flask that was in the oil bath pan. At the beginning of the experiment, the temperature of the oil bath pan was kept at 95ºC, and the PVA was completely dissolved after about 1.5 h. Then, PVP with a mass of 4.9 g was added when the solution was cooled to 60ºC, and the solution was stirred at constant temperature until completely dissolved. Zeolite with a mass of 3.5 g was added to the water-based copolymer solution for mixing and stirring for 1 h. Finally, the epoxy resin with a mass of 14 g was added to the mixed solution and reacted for 2 h to obtain the membrane solution. Take 20 ml of membrane solution and dry it in an incubator to form a membrane.

Experimental Design and Methods

Three levels of soil moisture W were set in the experiment: W_{60}, W_{80}, and W_{100}, which were 60%, 80%, and 100% of field water capacity, respectively. Three levels of soil temperature T were set: T_{15}, T_{25}, and T_{35}, which were 15ºC, 25ºC, and 35ºC, respectively. A comprehensive experimental design was used with nine treatments. The experimental soil with a mass of 2.5 kg was put into a polypropylene square box with

Author Copy • Author Copy • Author Copy • Author Copy • Author Copy • Author Copy • Author Copy • Author Copy • Author Copy • Author Copy

the same parameters, and the soil depth was set to 8cm. The self-made composite membrane material was dried to a constant weight and cut into a square with a size of 3×3 cm. The membrane materials with a mass of 1.125 g were buried in the soil with different moisture contents and put into the incubator at different temperatures. The burial depth of the membrane materials in the soil was set to 5 cm. During the test, water was replenished regularly to ensure that the soil water content was at the set level. After the membrane material was degraded for a certain period of time, it was dried in a vacuum to determine its weight at a constant weight.

Experimental Setup Parameters

The experimental setup parameters were as follows: polypropylene square box, length, 15 cm; depth, 10 cm; density, 0.89-0.91 g/cm^3; fusing point, 164-170ºC; tensile strength, 25-39 Mpa; elongation at break, 200-400%, constant temperature biochemical incubator (SPX-350BE), rated voltage, 220V/50HZ; rated power, 800W; temperature control range, 0-70ºC; temperature control accuracy, 0.1ºC.

Measurement Items and Methods

The degradation rate of membrane material G (%) refers to previous determination methods [17] and is calculated by formula (1). The molecular structure and chemical composition of the membrane material were analyzed by infrared spectroscopy [18]. The morphology of degraded membrane materials was photographed by SEM [19].

$$G = \frac{M_0 - M_1}{M_0} * 100\% \quad (1)$$

M_0 and M_1 were the masses of the sample to be tested prior to and after degradation.

Data Sample Processing

Microsoft Office 365 was used for data processing and table drawing. Origin 2019b was used for graph drawing, and a soil hydrothermal coupling model of membrane degradation rate was built based on 1 stop 8.0. The variance analysis of degradation characteristics of membrane materials under different soil hydrothermal conditions was conducted using IBM SPSS Statistics 22.

Result Analysis

Dynamic Changes in Membrane Degradation with Time under Different Hydrothermal Conditions

TThe dynamic curve of membrane degradation rate under different soil hydrothermal conditions is shown in Fig. 1. As shown in Fig. 1, the degradation rate of membrane materials was slow at first, and the degradation rate of membrane materials under different soil hydrothermal conditions differed little. At 30 days, the degradation rate of membrane materials under various treatments was 0.81%~0.97%. When the embedding time reached 40 days, the degradation rate of the membrane material began to significantly increase, indicating that as the embedding time increased, the internal structure of the membrane material was gradually destroyed and began to degrade significantly. The degradation rate of membrane materials under different soil, water, and heat conditions began to differ greatly between 50 and 80 days, with the difference reaching a maximum at 80 days. Under different soil, water, and heat conditions, the degradation rate

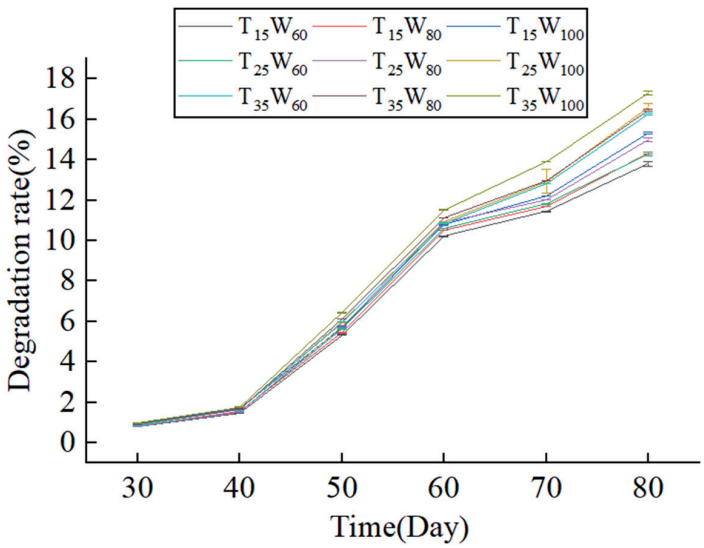

Fig. 1. Dynamic curve of membrane degradation rate under different soil hydrothermal conditions.

Author Copy • Author Copy • Author Copy • Author Copy • Author Copy • Author Copy • Author Copy • Author Copy • Author Copy • Author Copy

of membrane materials reached a minimum of 13.7% under $T_{15}W_{60}$ treatment and a maximum of 17.3% under $T_{35}W_{100}$ treatment.

Effects of Different Hydrothermal Conditions on Degradation Properties of Membrane Materials

Fig. 2 shows the degradation rate of membrane materials embedded in soil for 80 days under different hydrothermal conditions. As can be seen from Fig. 2, the quality of membrane materials in soil with different moisture temperatures all suffered a certain degree of loss. The degradation rate decreased by 13.7%-17.3% under different treatments, and the difference in the degradation rate under different treatments was 4.38%-26.28%. According to the mass loss rate and initial mass of membrane materials, the remaining mass of membrane material under different soil hydrothermal treatments was 0.154-0.195g. It showed that the degradation rate of membrane material varies greatly under different soil moisture and temperature conditions. It can also be seen from Fig. 2 that when the soil temperature was T_{15}, T_{25}, and T_{35}, the soil moisture content was increased from W_{60} to W_{100}, and the degradation rate of membrane materials monotonically increased by 11.68%, 15.97%, and 6.13%, respectively, indicating that the degradation rate of membrane material presents a positive response to the increase in water content, and the response was most obvious under T_{25}. In the condition of W_{60}-W_{100}, when the soil temperature was increased from T_{15} to T_{35}, the degradation rate of membrane material was monotonically increased by 18.98%, 15.38%, and 13.07%, respectively. This showed that the degradation rate of membrane material had a positive response to the increase in temperature, and the degradation rate had a stronger response to temperature when the moisture content was lower. It can be seen from the above analysis that there may be a certain interaction effect between soil moisture content and temperature on the degradation rate of membrane materials, so it is necessary to conduct a two-factor variance analysis on the data. Soil moisture and temperature on membrane materials have a significant influence on the degradation rate ($p<0.01$), but the interaction effect of influence on the degradation of membrane materials has not reached a significant level ($p>0.05$). The influence of *T*, *F*, and *T*F* on the degradation rate of membrane materials was as follows: *T>W>T*W*.

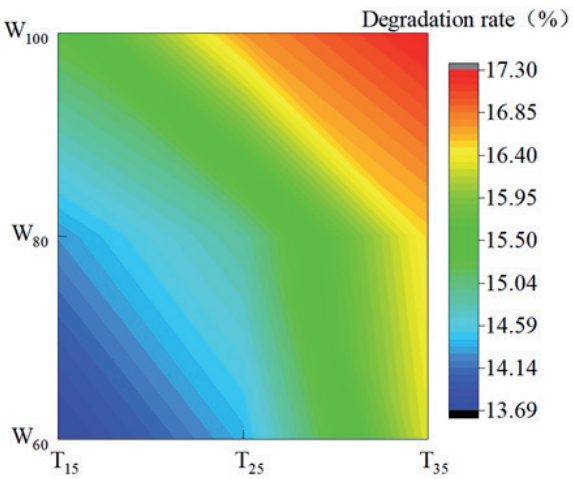

Fig. 2. Degradation rate of membrane under different soil hydrothermal conditions.

Degradation Model Construction

Fig. 3 shows the relationship between the degradation rate of membrane materials and hydrothermal factors. As can be seen from Fig. 3, the degradation rate of membrane materials under different treatments presents a monotonously increasing exponential change trend with the increase of temperature and water, which can be quantitatively described by using the single factor temperature model K (*T*) and water model K (*W*), respectively. It can also be seen from Fig. 3 that the determination coefficient R^2 of K (*T*) and K (*W*) single-factor degradation models was above 0.9, which indicated high fitting accuracy. However, the single factor model made it difficult to accurately describe the coupling effects of soil temperature and moisture on the degradation of membrane materials. In order to accurately describe the effects of various factors and their coupling effects on degradation rate, it was necessary to construct a hydrothermal coupling model of the degradation rate of membrane materials. Therefore, Equations (2) and (3) were multiplied to further establish the hydrothermal coupling model K (*T,W*) of membrane materials degradation.

$$K(T) = ae^{bt} \tag{2}$$

$$K(W) = ae^{cw} \tag{3}$$

$$K(T,W) = ae^{bt+cw} \tag{4}$$

Where a, b, and c are the model parameters, t is soil temperature, and w is soil moisture.

Table 1 shows the K (*T, W*) parameters of the degradation hydrothermal coupling model, and Fig. 4 shows the simulation effect of K (*T, W*). As can be seen from Table 1, the determination coefficient R^2 of K (*T, W*) was 0.927, which had a high fitting accuracy. As can be seen from Fig. 4a), degradation rate data samples were evenly distributed on both sides of the line, and the determination coefficient of the linear model formed by measured samples and calculated samples was 0.933, indicating that the predicted value of this model had a high degree of linear consistency with the measured value. It can also be seen from Fig. 4b) that the relative error of the model ranges from 0.13% to 3.48%, and the average relative error was 1.58%.

Author Copy • Author Copy • Author Copy • Author Copy • Author Copy • Author Copy • Author Copy • Author Copy • Author Copy • Author Copy

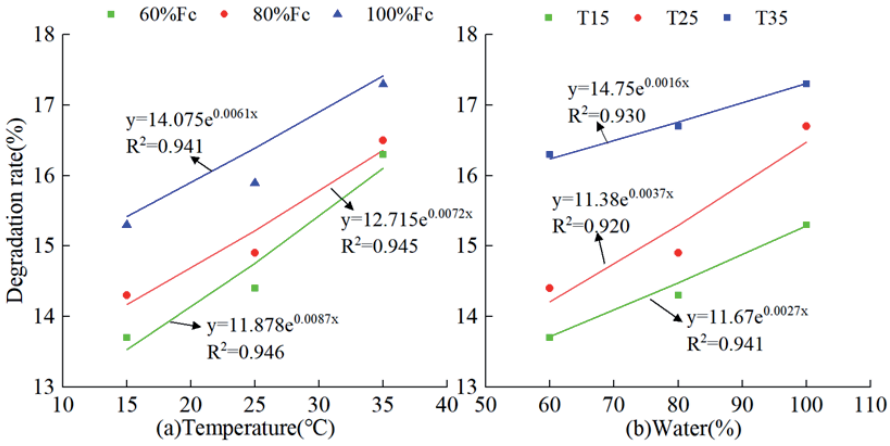

Fig. 3. Relationship between degradation rates and hydrothermal factors.

Table 1. Parameters of the hydrothermal coupling model.

Model parameter	a	b	c	R^2
	10.43	0.0026	0.0073	0.927

The error between the calculated value and the measured value was small.

Influence of Different Hydrothermal Conditions on Infrared Spectra of Membrane Materials

Fig. 5 shows the infrared spectra of different soils before membrane material degradation (CK) and after hydrothermal degradation. As can be seen from Fig. 5, the characteristic absorption peaks of the spectrum were mainly divided into two bands: 800~1500 cm^{-1} and 3000~3500 cm^{-1}. In the band of 800-1500 cm^{-1}, a narrow and strong absorption peak appeared in the characteristic region, and most of them presented a stepped-like pattern. In the band of 3000-3500 cm^{-1}, a strong and broad absorption peak appeared.The comparison of CK spectrum lines with the spectrum lines of membrane materials after degradation under different hydrothermal conditions showed that the positions of the maximum absorption peaks before and after degradation of membrane materials were basically the same, but the peak intensity of the same peak position had changed strongly, which indicated that the number of functional groups and the type of chemical bonds had changed after degradation of membrane materials, and a significant degradation phenomenon had occurred. The typical characteristic peaks of membrane materials before degradation include the -OH stretching vibration absorption peak near 3300cm^{-1} [20], the C=C absorption peak at 1500 cm^{-1}, the $-CH_2$ bond bending vibration peak at 1420 cm^{-1}, the C-C skeleton vibration absorption peak at 1092 cm-1, and the C-H stretching vibration peak at 2960 cm^{-1} [21]. Si-O stretching vibrations peak at 989 cm^{-1} [22]. Fig. 5 also showed that after membrane material degradation, the absorption peak of -OH stretching vibration became wider and stronger, while the absorption peak of C-H, $-CH_2$, and Si-O becomes

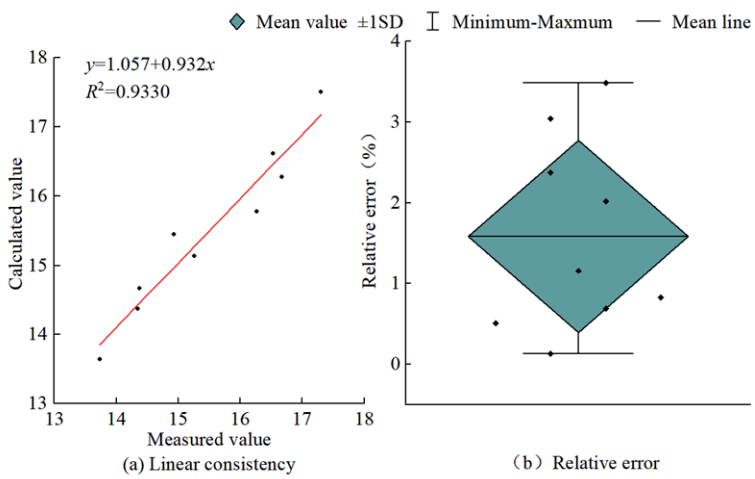

Fig. 4. Simulation effect of the hydrothermal coupling model on membrane degradation.

Author Copy • Author Copy • Author Copy • Author Copy • Author Copy • Author Copy • Author Copy • Author Copy • Author Copy • Author Copy

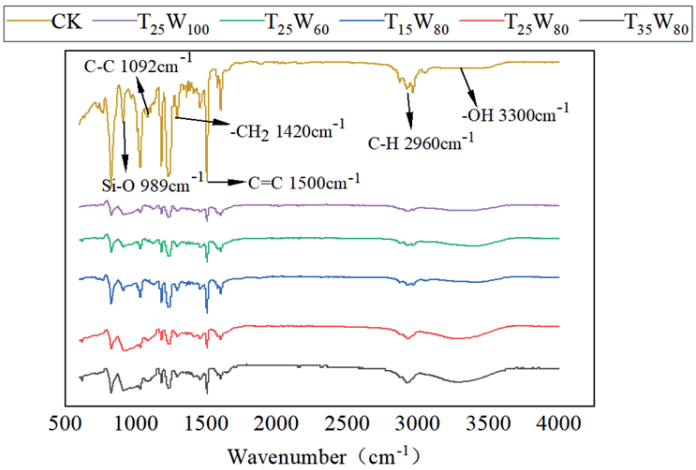

Fig. 5. Infrared spectra of membrane materials under different soil hydrothermal conditions.

stronger and weaker, and the peak of the C=C absorption peak appeared as a continuous step, indicating that the material structure of membrane materials changes and degradation occurs. When comparing $T_{15}W_{80}$, $T_{25}W_{80}$, and $T_{35}W_{80}$ spectrum lines, it can be seen that the absorption peak strength of -OH and C-H stretching vibration gradually increased with increasing temperature, indicating that when soil moisture is constant, the higher the temperature, the higher the degradation degree of membrane material. When comparing $T_{25}W_{60}$, $T_{25}W_{80}$, and $T_{25}W_{100}$ spectral lines, it can be seen that as the water content increases, the intensity of the C=C and Si-O absorption peaks decreases, indicating that the higher the soil temperature, the greater the degradation degree of the membrane materials.

The Effect of Different Hydrothermal Conditions on Membrane Micromorphology before and after Degradation

Fig. 6 shows the SEM images of membrane degradation under different soil hydrothermal conditions. As can be seen from Fig. 6, after the membrane material was embedded in the soil with different temperatures and moisture, the microscopic morphology changed to a great extent, with holes and cracks of different degrees appearing. It can also be seen from Fig. 6 that the surface treated by $T_{15}W_{60}$ was rough and raised, while the surfaces treated by $T_{15}W_{80}$ and $T_{15}W_{100}$ showed large cracks and holes. It shows that the increase in moisture at the same temperature will increase the degradation

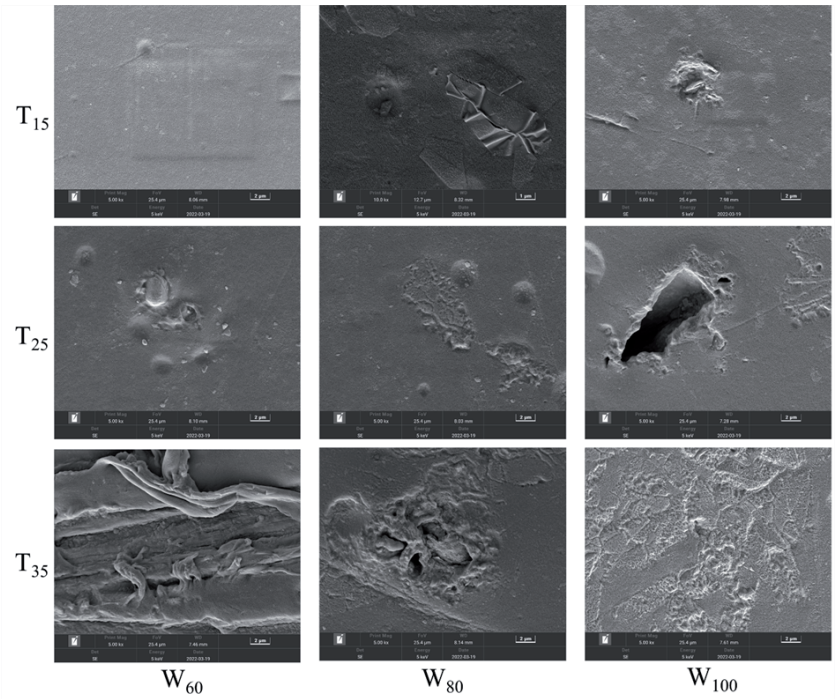

Fig. 6. Micromorphologies of membrane materials under different soil hydrothermal conditions.

Author Copy • Author Copy • Author Copy • Author Copy • Author Copy • Author Copy • Author Copy • Author Copy • Author Copy • Author Copy

degree of membrane material. The $T_{15}W_{80}$ treatment has small holes and cracks, and the holes on the surface of the $T_{25}W_{80}$ and $T_{35}W_{80}$ treatments gradually increase, and the internal structure is damaged, indicating that, under the same moisture conditions, increasing the temperature will greatly increase the degradation degree of the membrane material. Huge cracks appear on the surface of $T_{35}W_{60}$, $T_{35}W_{80}$, and $T_{35}W_{100}$ treatments, with the $T_{35}W_{100}$ treatment having the most obvious cracks, and the surface has festered. This could be related to microbial activity in the soil, as microbial activity is highest under $T_{35}W_{100}$ conditions and membrane material degradation is strongest.

Disscussion

Biodegradable coating materials are environmentally friendly and pollution-free and can be degraded under natural conditions, which has gradually become the development trend of slow and controlled-release fertilizer coating materials [23-25]. The degradation of composite membrane materials depends largely on their composition and structure, and the essence of their degradation is the breaking of chemical bonds [26]. The polyvinyl alcohol chain structure contains a large number of hydroxyl groups, and the degradation of the hydroxyl group by microorganisms occurs in two ways [27]: one is to oxidize PVA through secondary alcohol oxidase, so that two adjacent hydroxyl groups of PVA form an ß-dione structure; the other is to oxidize one hydroxyl group of PVA to form an ß-hydroxyl one. PVP had good binding with PVA. There are highly polar amide groups in the pyrrolidone ring, non-polar methylene and methane groups in the ring and main chain, and the end of the molecule is terminated by hydroxyl [28]. The infrared spectra of the composite membrane materials showed typical functional groups and absorption peaks, and the peak strength of the functional groups changed significantly before and after degradation, which indicated that the chemical bonds in the membrane materials were broken and the membrane materials were degraded.

The degradation process of composite membranes prepared from different raw materials in soil was quite different. The degradation degree of composite membrane was found to be the highest when the temperature was 35ºC and the moisture content was 0.226 g/g, and the degradation rate reached 17.3% after 80 days of embedding. The degradation rate of polybutanediol succinate (PBS) modified cellulose acetate (CA) composite membrane prepared by Ghaffarian was about 12% after 80 days of burial at 30ºC [29]. After 80 days of burial at room temperature, the degradation rate of titanium dioxide (TiO_2), modified polyvinyl alcohol (PVA), and polylactic acid (PLA) composite membranes was approximately 33% [30]. Song prepared biodegradable materials with phosphorus-containing polybutylene succinate (P-PBS) and polylactic acid (PLA) as raw materials, and the degradation rate of the materials was about 19% in 90 days under the conditions of 24ºC buried soil temperature and 12 hours of light [31]. Table 2 shows the approximate degradation rates of four different composite membranes over time. As shown in Table 2, the degradation rates of composite membranes prepared from various raw materials vary greatly. The membrane materials prepared by predecessors conform to the trend of logarithmic type in the degradation process [29, 30], while the membrane materials in this paper conform to the S-shaped curve in the degradation process. PVA, PVP, and PLA contain hydrophilic groups such as -OH, -COOH, and lactam, which were easily affected by soil moisture during the degradation process [30, 32], whereas PBS was relatively hydrophobic and might be greatly affected by soil temperature [29], and the PBS modified by phenyl phosphoric acid further decreases the crystallinity and increases the polarity, and its degradation performance also changed greatly [31]. According to research, the polymer degraded quickly when the polymer's covalent bond was broken [33]. The covalent bond formed by PVA and PLA will form oligomers after ester cleavage, and oligomer formation is conducive to rapid degradation [30]. After combining PVA and PVP, hydrogen bonds were formed inside the molecule, and the presence of intermolecular hydrogen bonds caused the membrane material to be tightly bonded inside, resulting in a slow degradation rate of the membrane material during the initial embedding stage. With the extension of embedding time, the continuous action of temperature and soil enzymes will hydrolyze the hydrogen bond, accelerating the degradation rate of membrane materials (Fig. 7). The degradation of polymers in soils is influenced not only by temperature, moisture, and the number and type of microorganisms, but also by abiotic conditions such as light [34]. Light degradation was an important step in the polymer degradation process. When a polymer absorbs a series of light rays, the internal chemical bond is broken [35], and the electrons within the molecule are excited to a higher energy level after absorbing high-energy radiation, resulting in polymer oxidation and hydrolysis [36, 37]. In this paper, there was no influence of natural light in the degradation process of membrane materials, and the membrane materials prepared by Song were accompanied by 12 h of light during the degradation process [31]. In previous experiments, if

Table 2. Approximate degradation rate of different composite membranes under specific time.

Time	30	40	60	80
PVA/PVP/zeolite	0.97%	1.75%	11.53%	17.3%
PBS/CA	2.3%	4.1%	9.4%	12.1%
PVA/PLA/ TiO_2	12.4%	23.4%	28.7%	33.1%
P-PBS/PLA	4.8%	7.1%	12.5%	18.2%

Author Copy • Author Copy • Author Copy • Author Copy • Author Copy • Author Copy • Author Copy • Author Copy • Author Copy • Author Copy

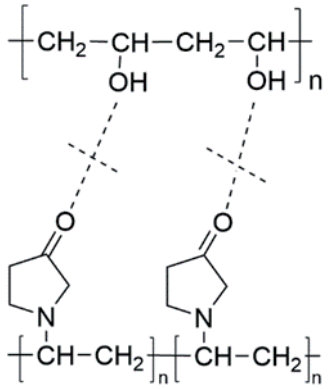

Fig. 7. Schematic diagram of the intermolecular hydrogen bond breakage.

the membrane materials were buried in shallow soil, there might be the influence of light [29, 30], which also causes the differentiation and degradation of membrane materials. pH also had a great impact on the degradation of materials. Jiang put the PO3G-PA/PLLA composite membrane into three buffers with different pH values and measured its degradation performance at 60ºC [38]. The results showed that the degradation rate of the membrane was faster in an alkaline environment. In this paper, natural soil with a pH of 8.43 was used for all treatments to better simulate the degradation law of materials in their natural state.

The degradation degree of membrane materials will be affected by soil temperature, moisture, and the number and type of microorganisms. The results showed that the degradation rate of membrane material in $T_{35}W_{100}$ soil was optimal. Zhao [39] discovered that when the soil temperature was 35ºC and the water content was 0.25 g/g, the membrane degradation rate was the fastest. The optimal degradation temperature was the same as described in this paper, but the optimal degradation water was slightly higher. According to the findings of Tian's research [40], the degradation rate of the seaweed polysaccharide membrane was greatest when the soil temperature was 25ºC, and the optimal degradation temperature obtained in this study was lower than that in this paper. The reasons for the above differences may be the different structure and composition of the membrane material and the different growth responses of soil microorganisms to temperature. The membrane structure of Zhao [39] was mainly starch and polyvinyl alcohol, while that of Tian [40] was a linear block copolymer composed of seaweed polysaccharides. In this paper, the structure of the composite membrane is a three-dimensional copolymer structure of PVA and PVP chemical crosslinking and zeolite physical blending. The different composition and structure of the composite membrane will lead to a difference in its crosslinking density, which consequently leads to a difference in its degradation. A large number of studies have proved that soil microorganisms play an important role in the degradation of organic materials [41-44]. The membrane materials of Zhao [39] and this article are mainly PVA, and the dominant degrading strain is PVA-degrading bacteria, while the membrane material of Tian [40] is mainly seaweed polysaccharide, and the dominant degrading strain is seaweed polysaccharide-degrading bacteria. Previous studies showed that the optimum growth temperature of the PVA-degrading strain Pseudomonas XT11 was 30ºC [45]. The optimum growth temperature of polysaccharides degrading strain L206 was 25ºC [46], and the optimum growth temperature of the PVA degrading strain was significantly higher than that of the Pseudomonas Pachastrellae degrading strain. The different optimum growth temperatures of the degrading strain resulted in the differentiation of the degradation conditions of membrane materials.

Conclusions

(1) The degradation degree in the membrane material showed a positive response to the increase in temperature and moisture. Soil moisture and temperature on membrane materials had a significant influence on the degradation rate ($p<0.01$), but the interaction effect on the degradation of membrane material was not significant ($p>0.05$).

(2) The K (T, W) determination coefficient R^2 of the hydrothermal coupling model reached 0.927, and the average relative error of linear fitting was 1.58%, which indicated that the model fitting effect was good.

(3) The infrared spectrum showed that the absorption peak of the -OH stretching vibration became wider and stronger after degradation, while the absorption peak of C-H, $-CH_2$, and Si-O became weaker, and the peak of the C=C absorption peak appeared as a continuous step after degradation. SEM electron microscopy showed that there were different degrees of degradation in each treatment, and the degradation of $T_{35}W_{100}$ was the highest.

Acknowledgments

This research is financed by the National Natural Science Foundation Program of China (51909184) and the China Postdoctoral Science Foundation (2020M670693).

Conflict of Interest

The authors declare no conflict of interest.

References

1. JIANG Z., YANG S., CHEN X., PANG Q., XU Y., QI S., DAI H. Controlled release urea improves rice production

Author Copy • Author Copy • Author Copy • Author Copy • Author Copy • Author Copy • Author Copy • Author Copy • Author Copy • Author Copy

and reduces environmental pollution: A research based on meta-analysis and machine learning. Environmental Science and Pollution Research, **29**, 3587, **2022**.

2. QIAO D., LIU H., YU L., BAO X., SIMON G. P., PETINAKIS E., CHEN L. Preparation and characterization of slow-release fertilizer encapsulated by starch-based superabsorbent polymer. Carbohydrate polymers, **147**, 146, **2016**.
3. LU P., ZHANG Y., JIA C., LI Y., ZHANG M., MAO Z. Degradation of polyurethane coating materials from liquefied wheat straw for controlled release fertilizers. Journal of Applied Polymer Science, **133** (41), **2016**.
4. MARCINCZYK M., OLESZCZUK P. Biochar and engineered biochar as slow-and controlled-release fertilizers. Journal of Cleaner Production, **339**, 130685, **2022**.
5. AZEEM B., KUSHAARI K., MAN Z.B., BASIT A., THANH T.H. Review on materials & methods to produce controlled release coated urea fertilizer. Journal of controlled release, **181**, 11, **2014**.
6. LAWRENCIA D., WONG S.K., LOW D.Y.S., GOH B.H., GOH J.K., RUKTANONCHAI U.R., TANG S.Y. Controlled release fertilizers: A review on coating materials and mechanism of release. Plants, **10** (2), 238, **2021**.
7. ABHIRAM G., BISHOP P., JEYAKUMAR P., GRAFTON M., DAVIES C.E., MCCURDY M. Formulation and characterization of polyester-lignite composite coated slow-release fertilizers. Journal of Coatings Technology and Research, **20**, 307, **2023**.
8. YE H., LI H., WANG C., YANG J., HUANG G., MENG X., ZHOU Q. Degradable polyester/urea inclusion complex applied as a facile and environment-friendly strategy for slow-release fertilizer: Performance and mechanism. Chemical Engineering Journal, **381**, 122704, **2020**.
9. YU X., WANG Z., LIU J., MEI H., YONG D., LI J. Preparation, swelling behaviors and fertilizer-release properties of sodium humate modified superabsorbent resin. Materials Today Communications, **19**, 124, **2019**.
10. NAGARKAR R., PATEL J. Polyvinyl alcohol: A comprehensive study. Acta Scientific Pharmaceutical Sciences, **3** (4), 34, **2019**.
11. SUN H., LEI T., LIU J., GUO X., LV J. Physicochemical Properties of Water-Based Copolymer and Zeolite Composite Sustained-Release Membrane Materials. Materials, **15** (23), 8553, **2022**.
12. KASSEM I., ABLOUH E.-H., EL BOUCHTAOUI F.-Z., KASSAB Z., HANNACHE H. SEHAQUI H., EL ACHABY M. Biodegradable all-cellulose composite hydrogel as eco-friendly and efficient coating material for slow-release MAP fertilizer. Progress in Organic Coatings, **162**, 106575, **2022.**
13. VAN SPEYBROECK V., HEMELSOET K., JOOS L., WAROQUIER M., BELL R.G., CATLOW C.R.A. Advances in theory and their application within the field of zeolite chemistry. Chemical Society Reviews, **44** (20), 7044, **2015**.
14. LONG S.F., ZHU Q.H., ZHOU J.L., HUANG D.Y., LIU B., LV G.H., DUAN M.M. Degradation of the bast fiber mulching film under different soil moisture conditions. Research of Agricultural Modernization, **40** (02), 349, **2019** [In Chinese].
15. ZHANG K., XU J., ZHANG M. Degradation behavior of PPC/PBS as urea coating in soil. Journal of Plant Nutrition and Fertilizers, **21** (03), 624, **2015** [In Chinese].
16. IRFAN S.A., RAZALI R., KUSHAARI K., MANSOR N., AZEEM B., VERSYPT A.N.F. A review of mathematical modeling and simulation of controlled-release fertilizers. Journal of controlled release, **271**, 45, **2018**.
17. SONG J., ZHAO H., ZHAO G., XIANG Y., LIU Y. Novel semi-IPN nanocomposites with functions of both nutrient slow-release and water retention. 1. Microscopic structure, water absorbency, and degradation performance. Journal of agricultural and food chemistry, **67** (27), 7587, **2019**.
18. WANG Z., YU H., XIA J., ZHANG F., LI F., XIA Y., LI Y. Novel GO-blended PVDF ultrafiltration membranes. Desalination, **299**, 50, **2012**.
19. LI J., LIU Y., LIU J., CUI X., HOU T., CHENG D. A novel synthetic slow release fertilizer with low energy production for efficient nutrient management. Science of the Total Environment, **831**, 154844, **2022**.
20. HEMALATHA K., SOMASHEKARAPPA H., SOMASHEKAR, R. Microstructure. AC conductivity and spectroscopic studies of cupric sulphate doped PVA/PVP polymer composites. Advances in Materials Physics and Chemistry, **5** (10), 408, **2015**.
21. CHOUDHARY S. Characterization of amorphous silica nanofiller effect on the structural, morphological, optical, thermal, dielectric and electrical properties of PVA–PVP blend based polymer nanocomposites for their flexible nanodielectric applications. Journal of Materials Science: Materials in Electronics, **29** (12), 10517, **2018**.
22. LIU F.J., WU H.L., WEI Q.Y., LI D.C., SU L. Adsorption of Phenolic Acids from Sucrose Solution on Chitosan Modified Zeolite. Modern Food Science and Technology, **37** (05), 180, **2021** [In Chinese].
23. JIN S., WANG Y., HE J., YANG Y., YU X., YUE G. Preparation and properties of a degradable interpenetrating polymer networks based on starch with water retention, amelioration of soil, and slow release of nitrogen and phosphorus fertilizer. Journal of Applied Polymer Science, **128** (1), 407, **2013**.
24. MURUGAN P., ONG S.Y., HASHIM R., KOSUGI A., ARAI T., SUDESH K. Development and evaluation of controlled release fertilizer using P (3HB-co-3HHx) on oil palm plants (nursery stage) and soil microbes. Biocatalysis and Agricultural Biotechnology, **28**, 101710, **2020**.
25. WANG X., LV S., GAO C., XU X., WEI Y., BAI X., WU L. Biomass-based multifunctional fertilizer system featuring controlled-release nutrient, water-retention and amelioration of soil. RSC advances, **4** (35), 18382, **2014**.
26. HSU S.-T., TAN H., YAO Y.L. Effect of excimer laser irradiation on crystallinity and chemical bonding of biodegradable polymer. Polymer Degradation and Stability, **97** (1), 88, **2012.**
27. KAWAI F., HU X. Biochemistry of microbial polyvinyl alcohol degradation. Applied microbiology and biotechnology, **84**, 227, **2009**.
28. KOCZKUR K.M., MOURDIKOUDIS S., POLAVARAPU L., SKRABALAK S.E. Polyvinylpyrrolidone (PVP) in nanoparticle synthesis. Dalton transactions, **44** (41), 17883, **2015**.
29. GHAFFARIAN V., MOUSAVI S.M., BAHREINI M., AFIFI M. Preparation and characterization of biodegradable blend membranes of PBS/CA. Journal of Polymers and the Environment, **21**, 1150, **2013**.
30. ALI H.E., ELBARBARY A.M., ABDEL-GHAFFAR A.M., MAZIAD N.A. Preparation and characterization of polyvinyl alcohol/polylactic acid/titanium dioxide nanocomposite films enhanced by γ-irradiation and its antibacterial activity. Journal of Applied Polymer Science, **139** (24), 52344, **2022**.

Author Copy • Author Copy • Author Copy • Author Copy • Author Copy • Author Copy • Author Copy • Author Copy • Author Copy • Author Copy

31. SONG J., ZHANG R., LI S. G., WEI Z.Q., LI X. Properties of phosphorus-containing polybutylene succinate/polylactic acid composite film material and degradation process effects on physiological indexes of lettuce cultivation. Polymer Testing, **119**, 107921, **2023**.
32. KOUSER S., PRABHU A., PRASHANTHA K., NAGARAJA G., D'SOUZA J.N., NAVADA K.M., MANASA D. Modified halloysite nanotubes with Chitosan incorporated PVA/PVP bionanocomposite films: Thermal, mechanical properties and biocompatibility for tissue engineering. Colloids and Surfaces A: Physicochemical and Engineering Aspects, **634**, 127941, **2022**.
33. IZDEBSKA J. Aging and degradation of printed materials. Printing on Polymers, pp. 353, **2016**.
34. LAWRENCIA D., CHUAH L.H., SRIKHUMSUK P., POH P. E.Biodegradation factors and kinetic studies of point-of-use water treatment membrane in soil. Process Safety and Environmental Protection, **161**, 392, **2022**.
35. SUN J., XIN X., SUN S., DU Z., YAO Z., WANG M., JIA R. Experimental and theoretical investigation on degradation of dimethyl trisulfide by ultraviolet/peroxymonosulfate: Reaction mechanism and influencing factors. Journal of Environmental Sciences,**127**, 824, **2023**.
36. SINGH B., SHARMA N. Mechanistic implications of plastic degradation. Polymer degradation and stability, **93** (3), 561, **2008**.
37. AL-SALEM S. Influence of natural and accelerated weathering on various formulations of linear low density polyethylene (LLDPE) films. Materials & Design, **30** (5), 1729, **2009**.
38. JIANG D.B., SONG X.S., MA M.N., HUAYING A., LU J.M., ZI C.L., ZHAO W., LAN Y.Z.,YUAN M.W. Preparation and Performance Study of Poly (1,3-propanediol) Ester/PLLA Blended Membrane. COATINGS, **13** (4), **2023**.
39. ZHAO A.Q. . The effects of soil moisture and temperature on the degradation of biodegradable Plastic film sand its field application. China Agricultural University, **2006** [In Chinese].
40. TIAN F.F. Degradation characteristics re-search of full biodegradable dry algae poly-saccharides mulch. Ocean University China, **2015** [In Chinese].
41. SUZUKI T., ICHIHARA Y., YAMADA M., TONOMURA K. Some characteristics of Pseudomonas 0–3 which utilizes polyvinyl alcohol. Agricultural and Biological Chemistry, **37** (4), 747, **1973**.
42. QIAN D., DU G., CHEN J. Isolation and culture characterization of a new polyvinyl alcohol-degrading strain: *Penicillium* sp. WSH02-21. World Journal of Microbiology and Biotechnology, **20**, 587, **2004**.
43. MATSUMURA S., SHIMURA Y., TERAYAMA K., KIYOHARA T. Effects of molecular weight and stereoregularity on biodegradation of poly (vinyl alcohol) by Alcaligenes faecalis. Biotechnology letters, **16**, 1205, **1994**.
44. CHUNG J., KIM S., CHOI K., KIM J.-O. Degradation of polyvinyl alcohol in textile waste water by Microbacterium barkeri KCCM 10507 and Paenibacillus amylolyticus KCCM 10508. Environmental technology, **37** (4), 452, **2016**.
45. WANG N.Q., ZOU X.M., CHEN H.H. Study on Screening and Degradation Character of Degrading Bacterium for Polyvinyl Alcohol. Microbiology China, **199** (03), 364, **2008** [In Chinese].
46. LIN Q.Q., PAN C.L., JIANG X.M., ZHANG Z.L., SU M.C. Isolation and identification of a seaweed polysaccharide degrading bacteria strain. Microbiology China, **41** (11), 2208, **2014** [In Chinese].